Optimal Allocation and Control of EV Energy Storage in Microgrids

Bakhe Nleya
Department of Electronic Engineering Durban University of Technology Durban, South Africa
bakhen@dut.ac.za

Article History: Received: 11 January 2021; Revised: 12 February 2021; Accepted: 27 March 2021; Published online: 28 April 2021

Abstract: Next Generation smart grid (SG) systems blend legacy power system networks and the latest state-of-the-art ICT technologies to ensure the efficiency, robustness as well as reliability of the former (power systems). The duplex flow of both information and energy enhances energy supply and de-mand response, as well as SG-related innovative business-oriented applications and services. Renewable generators (RGs) and Electric Vehicles (EVs) are becoming prominent in any SG setup as they promote environmental friendliness. The presence of both necessitates the optimal allocation of dis-tributed renewable generation (DRG) and energy storage sys-tems (ESS) at both SG and microgrid (MG) levels. In that way, grid stability will be always ensured. The paper describes and discusses an optimized ESS deployment approach for serving EVs (as they are one of the largest consumers of stored energy) and DRGs. Careful consideration of the state of the ESS is also considered by developing and applying a dynamic capacity adjustment algorithm to deal with the none-smooth cost func-tions. The proposed cost function takes into consideration the operation as well as investment cost minimization concurrently. The matrix real-coded genetic algorithm (MRCGA) is used to minimize the cost function of the system while constraining it to meet the customer demand, as well as the security of the system overall. The computational simulation results are presented to verify the effectiveness of the proposed method. The electricity network model is simplified using a virtual subnode concept to alleviate the computational load burden of a node's agent. Simulation results demonstrate the feasibility and stability of this dispatch strategy. Overall, our proposed framework and obtained results set a benchmark for the realization of agent-based coordination algorithms to solve the optimal dispatch problem

Keywords: energy cooperative microgrids, energy storage system, smart grid

1. Introduction

Next Generation SGs will address power needs more efficiently without compromising environmental friendliness as they will be dominated mostly by the incorporation of DRG sources. The incorporation of ICT technologies in such systems facilitates two-way information as well as energy flows such that the overall demand and supply can be addressed more precisely and in the process stability of the grid is maintained. Injection of DRGs implies a dominance of fluctuatory overall grid power that must be evened out from time to time, thus in the process intricating overall grid power flow management. The fluctuations in the grid power (voltage) can lead to issues such as voltage instability, power factor quality degradation, high level of harmonics, and overall power grid system unreliability[1],[2]. The voltage stability can be partly addressed by the incorporation of energy storage systems (ESSs) to supply stabilizing power when the need arises. At MG level, normally an external source would supply the extra required stabilizing power. However, in islanded MGs, the fossil together with distributed generation (DR) may jointly be used to mitigate these fluctuations. Such an intervention may require careful economic consideration. Whereas fossil-based generation may have low capital costs (CAPEXs), however operational expenditures (OPEX) may often be considerably higher. Furthermore, most fossil-generating sources are directly associated with excessive carbon emissions, hence making them environmentally unfriendly. Some fossil-based sources such as diesel generators are often slow in reacting to sudden power lulls when compared to ESSs. However, the latter alone may not always sustain the required extra power demand, hence the need to capitalize on the power already stored in EVs [3]. The EV storage system may form part of the MG stored power and in this way, the additional vehicle-to-grid (V2G) storage acts as a low-cost energy buffering service in the MG. However, the power contributed by V2G storage is also intermittent in nature because of the random plug-in pattern of EVs.

Fig. 1. Key SG Components.

A block diagram of an isolated MG is illustrated in Figure 1. It primarily comprises several types of energy generating sources. In the setup of a MG, a primary consideration would be limiting the number of DRG sources and ESSs to reduce both capital and operational expenditures. Increasingly, existing power grids are taking the SG approach and in the process the centralized generation that characterizes the traditional systems is now being taken over by DRG. The share of DRG is expected to increase. The injection of renewables at larger scales will cause more intermittency on the aggregated generation and thus resulting in bigger challenges in balancing tradeoffs between generation and demand. The renewable generation at consumer ends will normally utilize dc-ac converters whose power factors are close to unity, whereas that of the main grid is normally far less than that. This mismatch will lead to a deterioration of the power factor as viewed by the grid as it meets the consumer reactive power and only a fraction of active power. On the load side, increasingly, plug-in EVs will be injected into the grid and this influences the load.

2. Related Works

The incorporation of DRG, as well as the use of EV energy storage systems, has the potential to ensure grid frequency stability, reliability as well as overall optimal energy demand and supply balancing. A key performance indicator of the MG is in its ability to guarantee the supply of power at the correct power factor to all consumers. The intermittency can be minimized by the intervention of ESS and V2G contributions. The latter, however, also contributes to intermittency because of the random plug-in patterns coupled with mobility issues of EVs. However, the mobility and plug-in patterns can be modeled probabilistically and used to estimate the available power capacity at any time. To further lessen the unpredictabilities of the plug-and-play, a contractual obligation between the EV owner and MG may be necessary as proposed in several works. On one hand, the EV owner declares his immediate and near-future power usages and the MG accordingly will guarantee certain profit margins or penalties for any violations. It is therefore important that more research should focus on the operational planning of the V2G integrated MG.

A dynamic scheduling approach for charging/discharging of EVs using renewable sources, based on the load forecasting model is explored in [4] to estimate V2G storage at any given time. They use this model to ascertain the state of charge of the EV battery before its departure and consequently, it becomes easier to estimate the remaining V2G power.

The work in [5] uses the cumulative pdf of the plug-in pattern to estimate the power capacity at any given time. It also categorizes both EVs and all penalty functions accordingly. In that way, the profit function is maximized. The authors in [6] categorized the EV plug-in possibilities into car parks at offices, recreational places, and homes. They further modeled the mobility of trip chains and driving pattern profiles based on the surveyed data. They deduce the car parks at offices and homes as having the likelihood of maximum plug-in availability.

A real-time smart charging algorithm designed to minimize charging from the grid as well as stabilizing its frequency (of the grid) is analyzed in [7]. The authors herein further propose an algorithm for the charging of EVs from renewable energy sources with consideration of V2G regulation services. A novel agent-based coordinated dispatch strategy is proposed in [8]. The authors emphasize RGs should provide at least a part of EVs' charging energy to maximize desirable environmental benefits. They further advocate for new approaches that will ensure that EVs are dispatched in coordination with renewable power generation. In that way, the concerns, and requirements of both EV users and the MG are addressed. Notably, the EV owners want to charge at lowered costs and at the same time be assured that they would be able to complete their respective journeys or at least terminate at a charging station.

Further improvement of overall utilization in the use of renewable sources is explored in several literatures e.g, [9],[10], [11], [12], . Overall, it is seen to be a key component in grid load leveling without polluting the environment. In all cases studied, the EV batteries are charged in an environmentally friendly manner, and in turn, the V2G directly provides the main grid operational support in the form of load leveling. With the proposed strategy, each energy generator (node) in the MG is represented by a software agent. The agent is only aware of the elements that are locally connected to it and it is confined to managing the dispatch of EVs and RGs connected to it based on information received from the agents of other nodes that are directly linked to it. In that way, the stability of the network is ensured, and all objectives of dispatch are best achieved.

Aware of a very large computational burden that could occur in a node's agent connecting with a great number of child nodes, a novel concept of a virtual sub-node is proposed to simplify the electricity network model to reduce this burden. Accordingly, the dispatch problem is formulated as a distributed multi-objective constrained optimization problem (DMOCOP) and then solved using a dynamic programming-based algorithm to derive an optimal set of dispatch actions for EVs and RGs within a distribution network [13]. The DMOCOP is developed from the distributed constraint optimization problem (DCOP) using an Analytic Hierarchy Process (AHP) to simultaneously take into account several different objectives of dispatch as discussed above [13], [14].

The proposed dispatch strategy is tested on a radial distribution network, for its stability, feasibility, and effectiveness at satisfying the requirements of both EV users and the grid. In practice, the aggregator, or the distribution network operator (DNO) is supposed to oversee this optimal dispatch problem.

The rest of this chapter is organized as follows. In Section III, we describe a functional MG network. This is followed by the proposed coordinated dispatch framework of EVs and RGs in Section IV. A performance evaluation is carried out in section V, followed by conclusions in Section VI.

3. Mg Basic Configuration

A. MG Model description

Figure 2(a), illustrates a simplified model of a MG that comprises n DRG sources, $DRG = \{g_1, g_2, ...g_n\}$, each generating power equalling $p_i \in RG_i$. The generated power is quantized in fixed unit steps to a maximum $p_i^{\max} \in Z^+$. The same MG also serves m EVs, $EV = \{ev_1, ev_2, ..., ev_m\}$ each of which when parked can either be charging (+) or discharging (-). The charging current mode can either be high(3), medium(2), or low(1). If not charging, the mode is (0). Therefore, for each EV_i, the dispatch mode is $\delta_i \in DM_i = \{-3, -2, -1, 0, 1, 2, 3\}$. For that reason, the dispatch mode also connects to the external grid via a common bus V_o. In the same model, each of the k nodes, $V = \{V_1, ..., V_k\}$ is represented as a bus and can exchange power with peers. At the same time, each node has its fixed loads, i.e EVs and RGs.

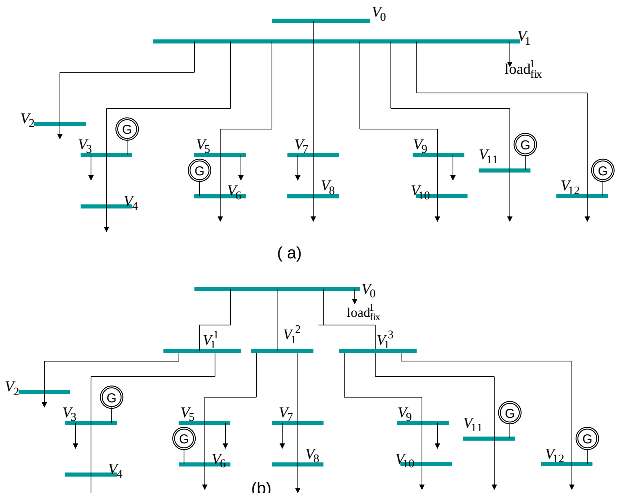

Figure 2. (a) Generic radial distribution network. (b) Same network with virtual sub nodes

Each main node V_i has child nodes $chi(V_i)$ as well as other nodes adjacent to it; $adj(V_i)$. Similarly, the fixed node at V_i is $load^i_{fix}$. The various nodes are also interconnected via distribution cables network. Thus $t_{i,j}$ denotes a distribution cable joining nodes i and j whose rated capacity is $C_{i,j}$ kVA.

Similarly, each node incorporates an agent that carries out the necessary information processing from its children before relaying them to the upstream node. As the MG grows in size, so would be the computational load, hence virtual sub-agents and nodes can share the computations. This is illustrated in Figure 2 (b). As seen from the same diagram, the node V_1 has three virtual sub-nodes V_1^1, V_1^2 and V_1^3 whose capacities are determined based on $C_{0,1}$ and $load^1_{fix}$. The load $load^1_{fix}$ remains connected to the parent node V_1.

$$load^1_{fix} = P\left[load^1_{fix}\right] + Q\left[load^1_{fix}\right] \tag{1}$$

The total active power transfer between V_1 and its children is:

$$P\left[C^n_{1,1}\right] = \frac{\sum\limits_{s \in child\left(V_1^n\right)} C_{s,1}}{\sum\limits_{d \in child(V_1)} C_{d,1}} \times P\left[load^1_{fix}\right] \times \frac{\left(C_{0,1} - \left|load^1_{fix}\right|\right)}{\left|load^1_{fix}\right|} \tag{2}$$

Whereas the reactive component transfer is;

$$Q\left[C^n_{1,1}\right] = \frac{\sum\limits_{s \in child\left(V_1^n\right)} C_{s,1}}{\sum\limits_{d \in child(V_1)} C_{d,1}} \times Q\left[load^1_{fix}\right] \times \frac{\left(C_{0,1} - \left|load^1_{fix}\right|\right)}{\left|load^1_{fix}\right|} \tag{3}$$

In the above two equations, n is virtual sub-cable indexing, whereas $\sum\limits_{d \in child(V_1^n)} C_{s,1}$ is the aggregate carrying capacity of cabling interconnecting the original node V_1 and child nodes $\sum\limits_{d \in child(V_1)} C_{d,1}$.

B. Optimal EV Charging and Discharging Model

In this section, we describe and analyze an optimized EV charging and discharging (dispatch) framework assumed in such a distributed MG power network system. In this regard, we first assume a finite unidirectional graph $\mathbf{W}(\mathbf{V},\mathbf{T})$ representing a set of generators(nodes) and cables. The associated set of power flows in the system is $\mathbf{F}$, $f_{i,j} \in \Re$ kW . The total carbon emissions by each generator in the system is ;

$$e_i = CI_i\, p_i \tag{4}$$

Where $CI_i \in \Re^+$ $kgCO_2 / kWh$ is its carbon emission rating.

The optimal dispatch goal in the allocation of power output focuses on:

$$\arg\min_{\alpha} \sum e_i = \sum_{i=0}^{n} CI_i\, p_i \tag{5}$$

This is subject to the following constraints:

Power flow along the distribution cable from node i to j may not exceed its designed (rated) capacity;

$$\left|f_{i,j}\right| \le t^c_{i,j} \tag{6}$$

Net power flow between nodes, and any node pair V_i and V_j must balance;

$$f_{i,j} = -t^c_{i,j} \tag{7}$$

Power conservation flow must always be true, i.e;

$$\sum_{\omega \in adj(V_i)} f_{\omega,i} + \sum_{l \in \mathbf{L}(V_i)} \beta_i + \sum_{g \in \mathbf{G}(V_i)} \alpha_g = 0 \tag{8}$$

Concerning the EV batteries, their state of charging (SOC) should be within limits $\lfloor 0,1 \rfloor$ i.e.:

$$0 < \mathrm{SOC} \leq 1 \quad (9)$$

To prolong the lifespan of the EV batteries, lengthy periods of over-discharge must be avoided as much as possible. For that reason, i.e., if SOC is currently close to the critical discharge voltage($SOC_{critical}$), the charging must commence immediately as a charging point is available.

$$SOC \approx SOC_{critical} \rightarrow \text{charging necessary} \quad (10)$$

4. Decentralized Optimal Dispatch

Having spelled out the optimal dispatch constraints in the previous section, we now describe a message passing technique based on the Decentralized Optimal dispatch (DoD) algorithm. Proof of its optimality is also provided. The algorithm is applied to the network provided in Figure 2 and it aims at maintaining low computational loads.

It is assumed that each node of the decentralized network has a single agent that processes all inbound and outbound messages as well as overall controlling the node. Each node in the exception of the root (V_o) may have one or several child nodes. Furthermore, each node is supplied from one or several generators each with its rated carbon intensity. Note that most RGs will have zero carbon intensity ratings. The matrix real-coded genetic algorithm (MRCGA) [15] is applied to minimize the cost function of the system while constraining it to meet the customer demand and security of the system.

The algorithm is in two phases namely, value computation (phase I) and value exchange (phase II).

Phase I: Value Computations

During this phase, an aggregated $energy\_\cos t$ message related to carbon emissions from a leaf node and its child nodes is generated and dispatched to the root node. An example $energy\_\cos t$ message from a child ($child(V_i)$) to its parent node V_i is typically an array;

$$\underrightarrow{energy\_\cos t_{child(v_i)\rightarrow V_i} \Rightarrow \lfloor flow\_CO_1,..., flow\_CO_y \rfloor} \quad (11)$$

The aggregated flow at the parent node side is directly dependent on the type of the individual generator sources as well as the magnitude of power each generates.

$$flow\_CO_i = \left\langle f_{child(i),i}\gamma(f_{child(i),i}) \right\rangle \quad (12)$$

where $f_{child(i),i\in\mathbf{Z}}\,\mathrm{kW}$ is the net energy flow along $t_{child(i),i}$ and $\left| f_{child(i),i} \leq t^{c}_{child(i),i} \right|$

γ is the aggregated carbon emissions from the node V_i and its children. Each calculated $flow\_CO$ element by V_i is mapped by the same node to an OPC_state that characterizes the power flow as well as carbon emissions from it and its child nodes. For each $energy\_\cos t$ message by V_i the corresponding $flow\_CO$ element is generated according to:

$$f_{child(i),i} = \sum_{l\in\mathbf{L}(V_i)} \beta_l + \sum_{g\in\mathbf{G}(V_i)} \alpha_g \quad (13)$$

The carbon emission γ of the $flow\_CO$ element is computed from:

$$\gamma(f_{child(i),i}) = \sum_{g\in\mathbf{G}(V_i)} \alpha_g CI_g \quad (14)$$

Each parent node V_i further uses the $energy\_\cos t$ send from its child nodes to generate a reply $energy\_\cos t$ to them. The $reply\_energy\_\cos t$ message is an indicator of the amount of power that is transferable between them, and is this also bounded by the transmission capacity of $t^{c}_{child(i),i}$ (linking them).

Algorithm I: To parent array at Leaf Node

$DM_i := \prod_{ev \in EV_i} DM_i^{ev};$
for each p_i in RG_i {
  for each δ_i in DM_i {
    $load_{ev} := EV\ energy\_cal(\delta_i, SOC_i, SOC_{critica});$
    $f_{child(i),i} := -load_{fixed} - load_{ev} + p_i;$
    $pec(f_{child(i),i}) := U(p_i, \delta_i);$
    $if\ (\min\ pec(f_{child(i),i}))$ {
      $PfPc(f_{child(i),i}\, pec(f_{child(i),i}));$
        $LinkToPfDstate(P_c, p_i, \delta_i);$
    }
  }
}
$Toparent();$
Send Toparent array to parent node V_i

In this regard, it should also compute the $flow\_CO_2$ that will result in the minimum carbon emission value by way of iterating through its various possible outputs to each $flow\_CO_2$ element from each of its children's $energy\_cost$ messages.

Algorithm II: To parent array at Leaf Node

$DM_i := \prod_{ev \in EV_i} DM_i^{ev};$
$ChildComtoParent := \prod_{c \in child(V_i)} Toparent_{c \to i};$
  for each p_i in RG_i {
  for each δ_i in DM_i {
    for each child PfP_c *in ChildComToparent* {
    $load_{ev} := EV_{powercal}(\delta_i, SOC_i SOC_{critical});$
$load_{ev} := -load_{fixed} - load_{ev} + p_i + \sum_{c \in child(V_i)} f_{c,i}$
    $pec(f_{child(i),i}) := U(p_i, \delta_i) + \sum_{c \in child(V_i)} pec(f_{ci});$
    $if\ (\min\ pec(f_{child(i),i}))$ {
      $PfPc(f_{child(i),i}\, pec(f_{child(i),i}));$
        $LinkToPfDstate(P_c, p_i, \delta_i);$
    }
  }
}
$Toparent();$
Send Toparent array to parent node V_i

In this case, a state representing a combination of a single $flow\_CO_2$ from each child and its output is computed according to:

$$f_{child(i),i} = \sum_{l \in \mathbf{L}(V_i)} \beta_l + \sum_{g \in \mathbf{G}((V_i)} \alpha_g + \sum_{c \in child(V_i)} f_{ci} \quad (15)$$

Algorithm III: Merging Power Cost Messages

$DM_i := \prod_{ev \in EV_i} DM_i^{ev};$
$ChildComtoParent := \prod_{c \in child(V_i)} Toparent_{c \to i};$
$\text{for each } \mathrm{p_i} \text{ in } RG_i \{$
$\text{for } \alpha_\mathrm{i} \leftarrow 0 \text{ to} genMax \{$
$for\ each\ child\ energy\_\cos t \{$
$rFlow \leftarrow \alpha_i + load + sum(OPCstate);$
$rCO_2 \leftarrow (\alpha_i + CI_i + sum(OPCState);$
$if\ (\min(rFlow, rCO_2))\{$
$energy\_\cos t(rFlow,\ rCO_2);$
$set\ new\ \min num(energy\_\cos t);$
$link\ to\ OPCState(energy\_\cos t, \alpha_i);$
$LinkToPfDstate(P_c, p_i, \delta_i);$
$\}$
$\}$
$\}$
$Send\ Toparent\ array\ to\ parent\ node\ \mathrm{V_i}$

Algorithm I is a summary pseudocode for the message construction from a leaf to the parent node. For the same algorithm, it can be noted that the computational load increases more or less linearly with RG maximum power output. This is explained by line codes 1 to 3.

If the same leaf node connects EVs, the associated computational load varies exponentially with their numbers. This is because the leaf node has to carry out iterations through all possible states relating to its RG power output values as well as individual EV's dispatch actions such as charging/discharging at low, moderate, or high currents.

Algorithm II provides a summary pseudo-code of a leaf node with children. Note that in this case, it iterates through the Cartesian product of its RG values, its EV dispatch actions, and as well as all its children's states. This is indicated by line codes (2-5)

Phase II: Propagation of Value

As explained in the preceding section, a root node solicits energy cost messages from all associated children, before computing the output demand power to sustain all active loads within the grid at minimized carbon emissions. In the actual implementation details, the root node's agent carefully examines and generates each possible permutation (combination) of $flow\_CO$ messages to determine whether the current load demands can be matched with the supply and which combination would result in minimal total penalty costs. Equations (10) to (12) in the preceding section are used to compute the resultant flow of a state. Only when the net power flow is zero, will the state of the network be considered feasible, and in that case the power supply balances with demand. As such, a combination will generally be regarded as feasible only when the required power flow from the root node to satisfy all corresponding loads within the network is within its given feasible domain. Thus, the optimum state of the network would be a feasible combination that minimizes the total penalty cost. Once this has been determined, the root's agent sends the corresponding power flow values to all the root node's children, telling them which of their messages minimizes the total penalty cost. The child retrieves the correct message that has the same power flow value as that received from the root node. The entire operations are summarized in Figure 3.

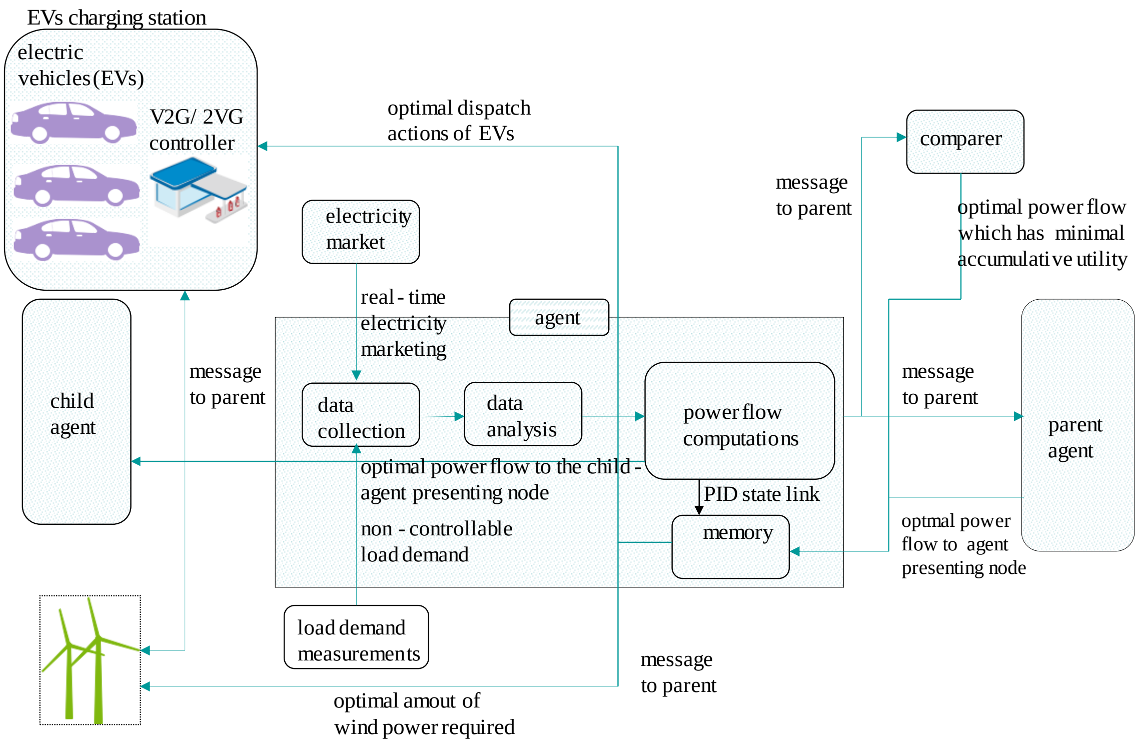

Figure 3. Summary operations at a root node's agent

The total number of messages that are handled by a node's agent varies linearly with the Microgrid's network size. This is partly summarized by Algorithm III. The messages include those sent as well as confirmations. Overall, the overall communication complexity is reciprocal to how many states converge to the same state.

5. Empirical And Simulation Evaluation

In this section, we carry out a brief empirical analysis followed by simulation performance evaluation of the proposed distributed coordinated dispatch framework of EV batteries as well as RGs. The distribution network which serves a total of 35000 EVs is shown in Figure 4. It comprises a total of 14 nodes. Five of the 14 nodes are RGs.

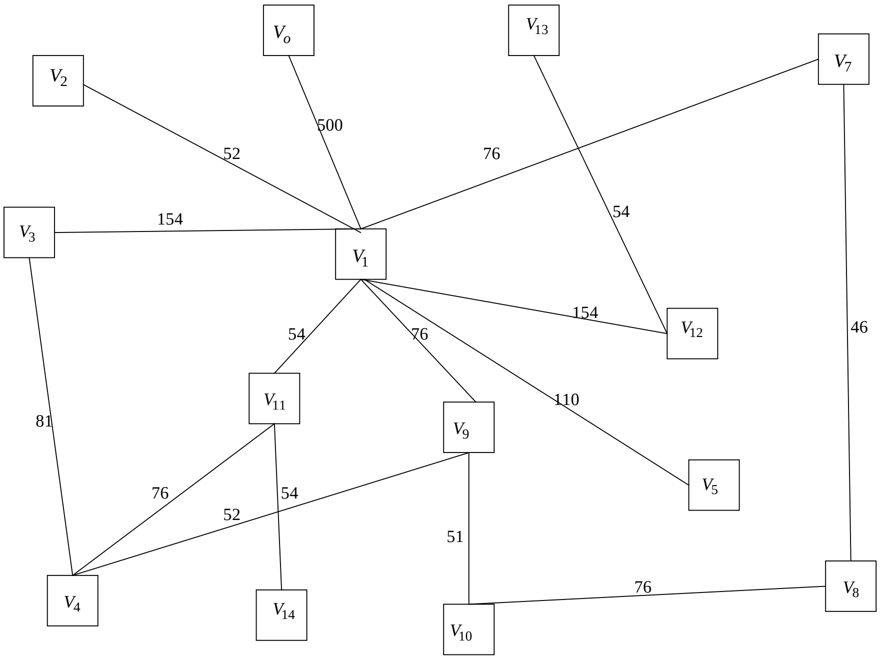

Figure 4. Distribution MG network

These are V_1, V_5, V_9, V_{11} and V_{14}. We will assume that each generating node is capable of directly connecting a maximum of 3500 EVs simultaneously to the microgrid. The transmission capacities (in MWs) of the interconnecting (distribution) cables are also indicated as well.

The fixed loads at each distribution node are tabulated in Table 1, below.

Table 1. Fixed loads at each distribution node

fixed loads		**node**
active (MW)	reactive ($MVAR$)	
39	11.3	V_1
23	9	V_2
56	4	V_3
36.5	10.1	V_4
25	5.5	V_5
55.5	6.2	V_6
18	0	V_7
13	2.29	V_8
12	0	$V9$
21	3.7	V_{10}
100	21.5	V_{11}
87	16.6	V_{12}
57	7.1	V_{13}
13	2.28	V_{14}

We start by carrying out an empirically comparative evaluation of the proposed scheme versus the traditional MAX-SUM Dispatch algorithm in terms of turnaround latencies as well as volume of exchanged messages. Summarily, the MAX-SUM Dispatch algorithm utilizes message passing to transmit the utility variables around the factor graph representation of the microgrid network. In this case, the messages are conveyed from variable to function and vice-versa as follows:

From function to variables:

$$R_{a\to b} = \min_{\frac{X_a}{b}} \left[U_a(X_a) + \sum_{b' \in B(a)\setminus b} Q_{b' \to a}\left(x_{b'}\right) \right] \quad (16)$$

In the reverse direction, i.e from variable to function;

$$Q_{a\to b} = \sum_{a' \in A(b)\setminus a} R_{a' \to b}\left(x_b\right) \quad (17)$$

In the last two equations $A(b)$ is a specified set of functions associated with the variable x_b. Similarly $B(a)$ is a set of variables associated with the function a. Under the circumstances ;

$$X_a \setminus b \equiv \left\{x_{b'} : b' \in B(a) \setminus b\right\} \quad (18)$$

As such, a max-sum message being dispatched from a function to a distribution cable variable is an indicator of the flow in the cable with its domain bounded by the capacity of the distribution cable.

In carrying out the empirical evaluation, we further assume that the microgrid network has several substations, all can connect to the main 14 nodes as well as child nodes. Each substation can connect up to 14 nodes simultaneously. Nodes are assigned random loads that are mostly uniform in nature, RGs, and CO_2 emission intensities. Each generator output level can be regulated up to 10 discrete levels, whereas each distribution cable's rated capacity is fixed.

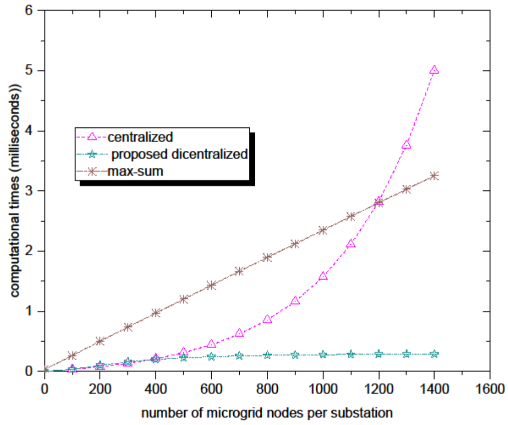

Figure 5. Turnaround (computational) time as a function of the number of nodes per substation

From Figure 5, it can be noted that both the centralized and proposed algorithms' computational time are initially quite low. However, as the number of connected nodes per substation exceeds 450, the centralized algorithm becomes sluggish, whereas the proposed algorithm still maintains fairly low computational time. Both the proposed and maximum-sum algorithms' computational times increase with the number of nodes connected. However, that of the maximum-sum increases rapidly and this is attributed to the additional unnecessary computations it carries out for infeasible variable states.

Similarly, if statistics of the total sum of messages exchanged are taken into account, we see that the proposed algorithm exchanges much fewer messages that the max-sum algorithm. As can be observed from Figure 6, the latter exchanges twice as many messages.

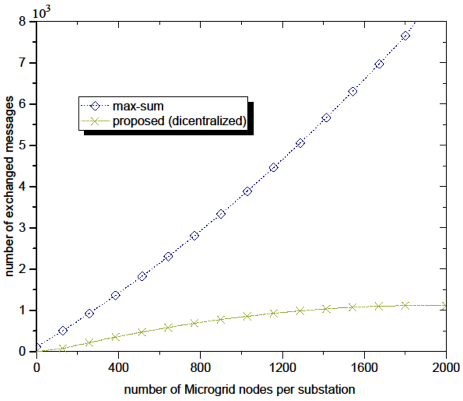

Figure 6. Total messages exchanged as a function of the number of nodes connected per substation**.**

Note that in Figure 5, the centralized computational times increase more less exponentially with the number of nodes connected per substation as is never aware of the overall network topology and always attempts to solve the combinatorial optimization by more standard approaches, such as the simplex method.

Overall, as more RGs are incorporated into the microgrid network, the centralized algorithm rapidly takes large turn around times to compute a solution to the optimal dispatch problem. On the other hand the proposed algorithm takes much lesser time and thus appropriate for coping with the ever increasing sizes of microgrids.

The proposed framework, i.e., of coordinated dispatching of EV battery charging is further simulated on the generic network of Figure 4 representing the modified distribution network of Figure 2(a) incorporating virtual sub nodes. Once again the number of RGs is limited to four and are represented in the simulation network of Figure 4 by nodes V_1 , V_5 , V_9 , V_{11} . The parameters of EV batteries are provided in table 2,[20]

Table 2 . Characteristics of E V battery in simulation

Type of battery	Capacity (Ah)	Rated time(hrs)	Peukert exponent	Effective available Capacity(Ah)
Lead acid	100	5 hrs	1.2	158.5
				114.87
				92.21

Table 3 cont . Characteristics of E V battery in simulation

Nominal Voltage(V)	Peukert Capacity	Discharge/charge Current p.u of C/5
240	182.06	0.1
		0.5
		1.5

The peak demand is experienced in the late afternoon and is about 358 MW and roughly conforms to that of local dial demand, Figure 7. We further assume that EV owners charge /or sell power according to the prevailing domestic tariffs. The RGs are all wind turbines and assumed to contribute a near constant aggregated power output to the grid daily.

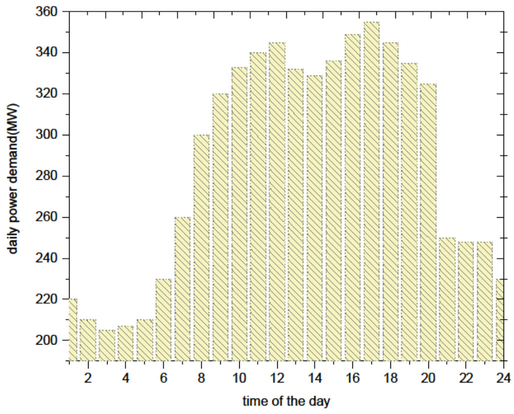

Figure 7. Aggregated fixed load demands on a single day

The population of all active EVs make an even but random travel pattern in the entire network. For that reason, in the simulation, their travel patterns are randomly generated in direct conformance to the assumed probability of parked cars during the week as shown in Figure 8.

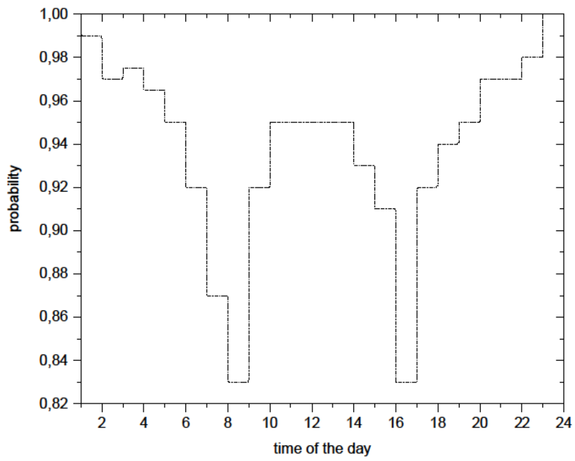

Figure 8. Probability of cars parked over a 24 hr period

When a given EV is in motion it is assumed to be discharging its EV battery by up to 20 amperes. The SOC are also randomly assigned such to curve a normal distribution function with mean $\mu = 0.655$ and deviation , $\sigma = 0.1$. All dispatch actions that take place are based on the dispatch strategy at the commencement of each time interval equaling 0.5 hours.

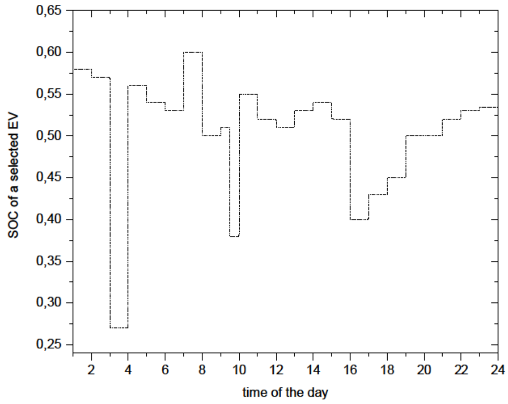

Figure 9. Typical daily variation of SOC of an EV

A typical daily SOC of an arbitrary EV is shown in Figure 9. To explain this in more detail, we select a single EV that we assume to be in use in the morning (08:00hrs to 10:00hrs) and evening (18:00hrs to 19:00hrs) daily throughout the week. This is depicted in Figure 10. For the rest of the day, the selected EV is parked, plugged into the grid for charging or for discharging power to the grid as part of the contracted V2G service.

To determine the daily costs to EV users, we repeated the simulation run several times, with each run commencing with a randomly chosen SOC. By comparison, it is generally observed that the average daily cost of each EV is lower when the charging is done in a controlled way. In this case, we assume recharging only commences when the SoC has dropped to 60% or less and that emphasis is put on the usage of renewable energy for charging as long as the distribution cables are not overloaded.

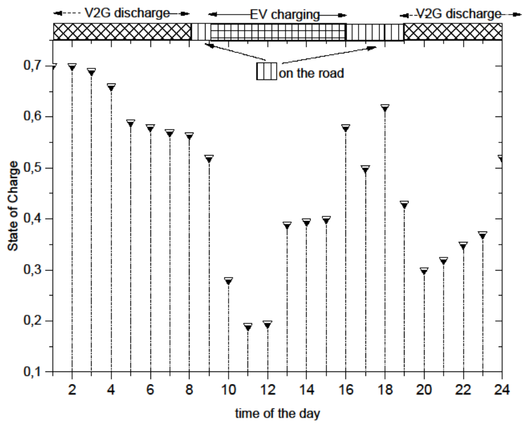

Figure 10. Single EV charging/ discharging

The simulation also confirms that the majority of the EVs can complete their daily journeys without running out of power on the highways (roads) and still retain the minimal 31% critical battery discharge threshold.

6. Conclusions

The proposed cost function takes into consideration the operation as well as investment cost minimization at the same time for the MG. The matrix real-coded genetic algorithm (MRCGA) is used to minimize the cost function of the system while constraining it to meet the customer demand and security of the system. The computational simulation results are presented to verify the effectiveness of the proposed method. The electricity network model is simplified using a virtual sub-node concept to alleviate the computation burden of a node's agent. Simulation results demonstrate the feasibility and stability of this dispatch strategy. Overall, our proposed framework and obtained results set a benchmark for the realization of agent-based coordination algorithms to solve the optimal dispatch problem in the smart grid

References

1. R. Chidzonga, M. Gomba and B. Nleya, "Energy Demand and Trading Optimization in Isolated Microgrids," 2020 Conference on Information Communications Technology and Society (ICTAS), Durban, South Africa, 2020, pp. 1-5, doi: 10.1109/ICTAS47918.2020.233994.
    A. Mutsvangwa, B. Nleya, M. Gomba and R. Chidzonga, "User and Microgrid Energy Optimization in Cooperative MGs," 2019 International Multidisciplinary Information Technology and Engineering Conference (IMITEC), Vanderbijlpark, South Africa, 2019, pp. 1-6, doi: 10.1109/IMITEC45504.2019.9015861.
2. S. Misra, P. K. Panigrahi and S. Ghosh, "Smart Battery Management Scheme for V2G Based EV Smart Charger – A Better approach of Allocation of EV Based Distributed Generation," 2020 IEEE International Symposium on Sustainable Energy, Signal Processing and Cyber Security (iSSSC), Gunupur Odisha, India, 2020, pp. 1-6, doi: 10.1109/iSSSC50941.2020.9358817.
3. A.-H. Mohsenian-Rad, V. W. Wong, J. Jatskevich, R. Schober, and A. Leon-Garcia, "Autonomous demand-side management based on game-theoretic energy consumption scheduling for the future smart grid," IEEE Transactions on Smart Grid, vol. 1,no. 3, pp. 320–331, 2010.
4. B.-G. Kim, S. Ren, M. van der Schaar, and J.-W. Lee, "Bidirectional energy trading and residential load scheduling with electric vehicles in the smart grid," IEEE Journal on Selected Areas in Communications, vol. 31, no. 7, pp. 1219–1234, 2013.
5. C. Joe-Wong, S. Sen, S. Ha, and M. Chiang, "Optimized day-ahead pricing for smart grids with device-specific scheduling flexibility," IEEE Journal on Selected Areas in Communications, vol. 30, no. 6, pp. 1075–1085, 2012.
6. A.-H. Mohsenian-Rad, V. W. Wong, J. Jatskevich, R. Schober, and A. Leon-Garcia, "Autonomous demand-side management based on game-theoretic energy consumption scheduling for the future smart grid," IEEE Transactions on Smart Grid, vol. 1,no. 3, pp. 320–331, 2010.
7. D. Gregoratti and J. Matamoros, "Distributed energy trading: the multiple-microgrid case," IEEE Transactions on Industrial Electronics, vol. 62, no. 4, pp. 2551–2559,2015.
8. U. k. Nath and R. Sen, "A Comparative Review on Renewable Energy Application, Difficulties and Future Prospect," 2021 Innovations in Energy Management and Renewable Resources(52042), Kolkata, India, 2021, pp. 1-5, doi: 10.1109/IEMRE52042.2021.9386520.
9. G. Zhang et al., "Forming a Reliable Hybrid Microgrid Using Electric Spring Coupled With Non-Sensitive Loads and ESS," in IEEE Transactions on Smart Grid, vol. 11, no. 4, pp. 2867-2879, July 2020, doi: 10.1109/TSG.2020.2970486.
10. R. F. Chidzonga and B. Nleya, "Perspectives On Impact of High Penetration of Renewable Sources on LV Networks," 2020 International Conference on Artificial Intelligence, Big Data, Computing and Data Communication Systems (icABCD), Durban, South Africa, 2020, pp. 1-5, doi: 10.1109/icABCD49160.2020.9183858.
11. R. Samu, M. Calais, G. Shafiullah, M. Moghbel, M. A. Shoeb and C. Carter, "Advantages and Barriers of Applying Solar Nowcasting in Controlling Microgrids: Findings From A Survey in 2020," 2020 International Conference on Smart Grids and Energy Systems (SGES), Perth, Australia, 2020, pp. 267-272, doi: 10.1109/SGES51519.2020.00054.
12. G. Shen, J. Zhuang, J. Yu, K. Xu and Y. Gao, "Micro Grid Scheduling Optimization Model Based on Multi-objective Genetic Algorithm," 2016 International Conference on Intelligent Transportation, Big Data & Smart City (ICITBS), Changsha, China, 2016, pp. 513-516, doi: 10.1109/ICITBS.2016.26.
13. B. Li, J. Wang and N. Xia, "Dynamic Optimal Scheduling of Microgrid Based on ε constraint multi-objective Biogeography-based Optimization Algorithm," 2020 5th International Conference on Automation, Control and Robotics Engineering (CACRE), Dalian, China, 2020, pp. 389-393, doi: 10.1109/CACRE50138.2020.9230079.
14. K. Christakou, J. LeBoudec, M. Paolone and D. Tomozei, "Efficient Computation of Sensitivity Coefficients of Node Voltages and Line Currents in Unbalanced Radial Electrical Distribution Networks," in IEEE Transactions on Smart Grid, vol. 4, no. 2, pp. 741-750, June 2013, doi: 10.1109/TSG.2012.2221751.
15. C. Chen, S. Duan, T. Cai, B. Liu and G. Hu, "Optimal Allocation and Economic Analysis of Energy Storage System in Microgrids," in IEEE Transactions on Power Electronics, vol. 26, no. 10, pp. 2762-2773, Oct. 2011, doi: 10.1109/TPEL.2011.2116808..